THERMOCATALYTIC CO_2-FREE PRODUCTION OF HYDROGEN FROM HYDROCARBON FUELS

Nazim Muradov
Florida Solar Energy Center
1679 Clearlake Road, Cocoa, FL 32922

Abstract

The main goal of this project is the development of an economically viable process for production of hydrogen and elemental carbon via thermocatalytic decomposition (TCD) of natural gas or other hydrocarbon fuels. The technical approach is based on a single-step decomposition (pyrolysis) of methane and other hydrocarbons over carbon-based catalysts in an air/water-free environment. This approach eliminates the concurrent production of carbon oxides and, therefore, obviates the need for water-gas shift and CO_2 removal stages, required by conventional processes (e.g., methane steam reforming and partial oxidation), which significantly simplifies the process. Considerable reductions in overall greenhouse gas emissions, compared to conventional processes, could also be expected from the TCD process. Clean carbon (free of sulfur, ash and metals) is produced as a valuable byproduct of the process. The experimental data on the catalytic activity of different carbon-based catalysts for the methane decomposition reaction are presented in this work. The paper also discusses factors affecting long-term stability of the carbon catalysts and the sustainability of the catalytic process. It was found that the process sustainability can be improved via in-situ generation of catalytically active carbon particles. Various conceptual designs for the reactor suitable for decomposition of methane with production of hydrogen-rich gas and continuous withdrawal of elemental carbon were considered; a fluidized bed reactor was selected as the most suitable for this purpose. The reactors for small-scale production of hydrogen (10 W and 1 kW range) have been designed, fabricated and tested. A wide range of hydrocarbon fuels, including methane, propane, gasoline and diesel fuel were converted into a hydrogen-rich gas with H_2 concentration up to 80 v.%, the balance being methane. The gas produced did not contain carbon oxides or other reactive

impurities, therefore, it could be directly fed to a fuel cell without need for the additional gas conditioning and purification stages. Techno-economic analysis conducted by NREL showed that the TCD process would be economically advantageous if credits for the carbon product and avoided CO_2 emissions were applied.

Introduction

Background and Overall Approach

Fossil fuels are likely to play a major role in hydrogen production in the near- to medium-term future. On the other hand, fossil fuels are major source of anthropogenic CO_2 emissions into the atmosphere. There are several possible ways to mitigate CO_2 emission problem. Among them are traditional (e.g. use of non-fossil and renewable energy resources), as well as novel technological approaches pertaining to fossil fuel decarbonization concept. Two fossil fuel decarbonization strategies are actively discussed in the literature: (i) hydrogen production by methane steam reforming coupled with CO_2 sequestration (fuel gas decarbonization), and (ii) hydrogen production via thermal decomposition (pyrolysis) of hydrocarbons with co-production of solid carbon (direct decarbonization of fuels). The following is a brief discussion of "fuel gas" and "direct" decarbonization strategies.

Figure 1 depicts the schematic diagram of fuel gas decarbonization (FGD) concept using natural gas (NG) as a feedstock. FGD system includes a methane steam reforming (SR) hydrogen production plant and a CO_2 sequestration subsystem.

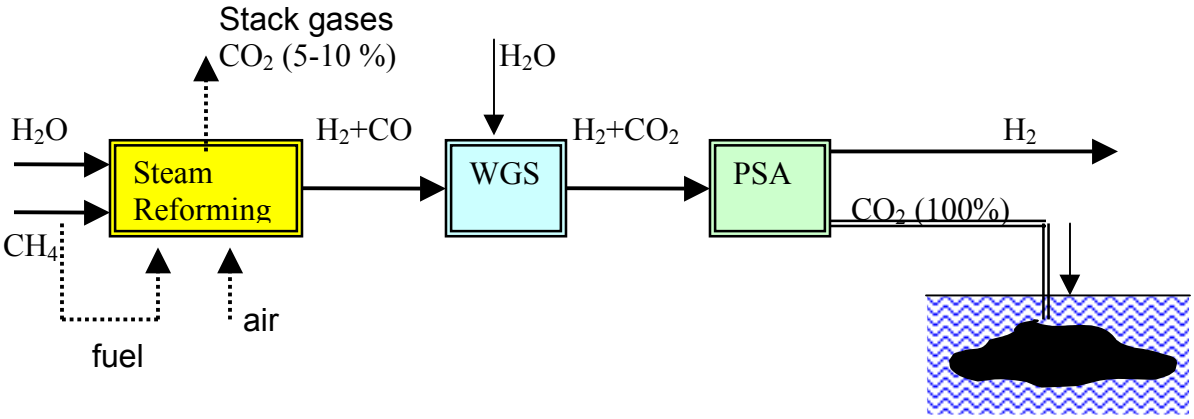

Figure 1. Schematic Diagram of a Fuel Gas Decarbonization Concept

The SR process consists of several stages: (i) highly endothermic catalytic steam reforming of methane (ΔH^o=206 kJ/mol), (ii) water-gas shift reaction (WGS), and (iii) separation of the H_2/CO_2 mixture (preferably, using a pressure swing adsorption unit, PSA). Other energy-intensive stages of SR process include: feedstock desulfurization and the production of steam

(average steam/carbon ratio of 3-5). As a result, a considerable part of NG (up to 30-35% of the total amount) is used as a process fuel, thus, producing significant amounts of stack gases with CO_2 concentration in the range of 5-10 v.%. Thus, SR process produces two streams of CO_2-containing gases: the concentrated stream after PSA (70% of the total) and diluted (stack gases) stream (30% of total) (Blok et. al 1997). The total CO_2 emissions (including stack gases) from SR process could reach up to 0.3-0.4 m^3 CO_2 per m^3 of hydrogen produced.

CO_2 sequestration involves the capture, pressurization, transportation and injection of liquid CO_2 under the ocean (at depths of more than 2 km) or underground (e.g. depleted NG wells, or geologic formations). All the operations associated with CO_2 sequestration are energy intensive and costly. There have been some estimates reported in the literature on the economics of CO_2 sequestration associated with hydrogen production from fossil fuels. Thus, according to the authors (Audus et.al. 1996), the capture and disposal of CO_2 add about 25-30% to the cost of hydrogen produced by SR. Furthermore, because of large energy consumption during CO_2 sequestration, additional amounts CO_2 will be emitted (0.25 kg CO_2 per kg of sequestered CO_2, assuming world average energy production scenario). The key risk factor of FGD approach results from uncertain long-term ecological consequences of CO_2 sequestration. Many questions with regard to the duration and extent of CO_2 retention (underground or under the ocean) still remain unanswered. There have been concerns expressed in the literature on possible hazardous environmental effects of CO_2 sequestration, e.g. the harmful effect of local decrease in pH on marine life (when disposing CO_2 in the ocean), or underground structural damage with catastrophic release of CO_2 (Steinberg 1999). Recent studies indicated that stockpiling CO_2 in plants and soil may be effective only for the short term, if at all (Perkins 2000).

Direct decarbonization (DD) strategy (see Figure 2) involves thermal decomposition (TD) (or cracking, pyrolysis) of methane and other hydrocarbons in air- and/or water-free environment with production of hydrogen and elemental carbon:

$$CH_4 \rightarrow C + 2H_2 \qquad \Delta H^o = 75.6 \text{ kJ/mole}$$

Methane decomposition reaction is moderately endothermic process. The energy requirement per mole of hydrogen produced (37.8 kJ/mole H_2) is somewhat less than that for the SR process. Due to a relatively low endothermicity of the process, less than 10% of the heat of methane combustion is needed to drive the process. Unlike FGD, the DD approach does not include WGS and CO_2 removal stages, which significantly simplifies the process. In addition to hydrogen as a major product, the process produces a very important byproduct: clean carbon. Carbon can be used as a commodity product or sequestered (or stored) for future use.

Kvaerner company of Norway has developed and operated plasma-assisted decomposition of methane into hydrogen and carbon black (Gaudernack et al. 1996). Although technologically simple, the process is energy-intensive: it was estimated that up to 1.9 kWh of electrical energy is consumed per one normal cubic meter of hydrogen produced (Fulcheri et al. 1995). Since 80% of the world electric energy supply is based on fossil fuels, electricity-driven hydrogen production processes (including electrolysis) generate large amounts of CO_2, and potentially would require its disposal.

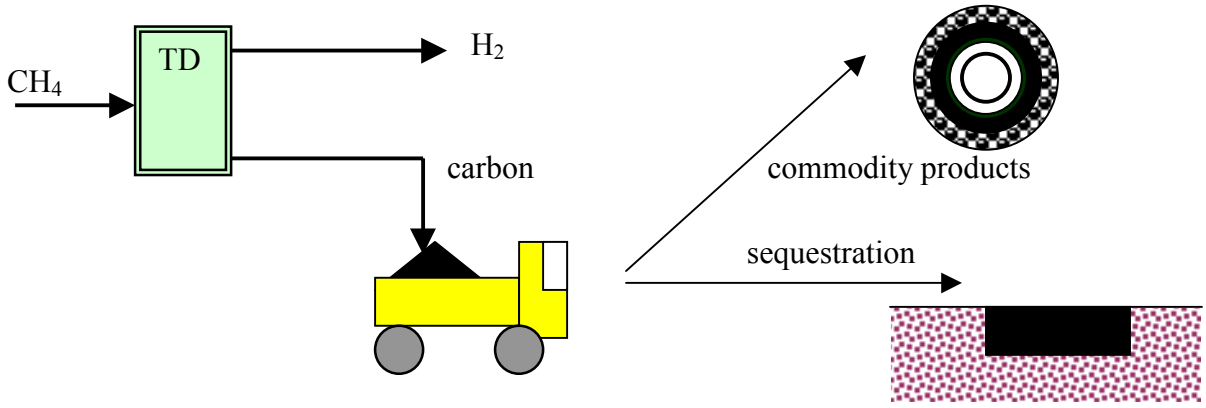

Figure 2. Schematic Diagram of a Direct Decarbonization Concept

There have been attempts to use different catalysts to reduce the maximum temperature of TD of methane. Metal catalysts, including Ni, Fe, Co and others, have been most commonly used for methane decomposition (Calahan 1974, Muradov 1993). However, there was a catalyst deactivation problem associated with the carbon buildup on the catalyst surface. In the vast majority of related publications (e.g., Calahan 1974, Pourier 1997) carbon produced was burned off the catalyst surface in order to remove it from the reactor and regenerate the original activity of the metal catalyst. As a result, the amount of CO_2 produced is comparable with that of the conventional processes (e.g., SR or partial oxidation). Another serious problem arising from the oxidative regeneration of metal catalysts relates to unavoidable contamination of hydrogen with carbon oxides, which would require an additional purification step.

Our technical approach is based on the use of carbon-based catalysts for hydrocarbon decomposition in an oxidant-free environment. Use of carbon catalysts offers the following advantages over metal catalysts: (i) no need for the regeneration of the catalyst by burning product carbon, (ii) no contamination of hydrogen with carbon oxides and, consequently, no need for the additional gas purification, and (iii) production of a valuable byproduct carbon. In Phase I work we demonstrated the technical feasibility of methane decomposition over carbon catalysts at moderate temperatures (<850^{o}C) with simultaneous production of hydrogen-rich gas and elemental carbon. Phase II work focuses on the improvement of long-term catalyst stability and process sustainability, and other technological aspects of the thermocatalytic process.

Experimental

Reagents

Methane (99.99 v.%, Air Products and Chemicals, Inc.) and propane (99.0 v.%, Praxair) were used without further purification. Samples of commercial gasoline and diesel fuel were purchased at a gas-filling station and dried over Drierite for two days before the experiments.

Samples of activated carbons were obtained from Barneby Sutcliffe Corp., NORIT Americas and Kanzai Coke & Chemicals. Cabot Corp. provided different samples of carbon black. Graphites, glassy carbon and acetylene black were obtained from Alfa Aesar and used without further purification. All carbon samples were used in the form of fine powder (<100μm). Table 1 summarizes the information on the carbon samples tested for catalytic activity in methane decomposition reaction.

Table 1. Carbon Catalysts Tested for Catalytic Activity in Methane Decomposition Reaction

Manufacturer (brand name) of carbon catalyst	Origin of carbon	Surface area, m^2/g	Method of activation of AC
NORIT Americas (Darco KB-B)	hardwood	1500	steam/chemical
NORIT Americas (Darco 20-40)	lignite coal	650	steam
NORIT Americas (Norit RO 0.8)	peat	900	steam
NORIT Americas (G-60)	proprietary	900	steam
Barnebey Sutcliff Corp. (CL-20)	coconut shell	1500	steam
Barnebey Sutcliff Corp. (KE)	coconut shell	1150	steam
Barnebey Sutcliff Corp. (GI)	coconut shell	1300	steam
Kanzai Coke & Chemicals (KCC) (MAXSORB MSP-15)	carbonized phenol resin	1980	KOH
KCC (MAXSORB MSP-20)	phenol resin	2260	KOH
KCC (MAXSORB MSC-25)	petroleum coke	2570	KOH
KCC (MAXSORB MSC-30)	petroleum coke	3370	KOH
Cabot (CB Black Pearls 2000)	petroleum	1500	
Cabot (CB Black Pearls 120)	petroleum	25	
Cabot (Vulcan XC72)	petroleum	254	
Cabot (Regal 330)	petroleum	94	
Acetylene Black	acetylene	80	
Diamond powder synthetic		7.9	
Graphite crystalline	petroleum coke	3-10	
Graphite microcrystalline	coke	10-12	
Graphite natural	graphite	4-6	
Glassy carbon			

Apparatus

The experimental set-up for hydrocarbon fuel decomposition consisted of 3 main subsystems: (1) a thermocatalytic reactor (with temperature-controlled electric heater and pre-heater), (2) a hydrocarbon metering and delivery sub-system, and (3) an analytical sub-system. All catalytic reactors were made out of fused quartz or ceramic (alumina) in order to reduce the effect of the reactor material on the rate of hydrocarbon decomposition. The reactor was maintained at a constant temperature via a type K thermocouple and Love Controls microprocessor. The amount of carbon catalyst used in the catalyst screening experiments varied in the range of 0.03-2.0 g. Hydrocarbon flow rates were metered by Gilmont flow meters and varied from 5 ml/min to 2

l/min (depending on the reactor used). Fused quartz tubings with the O.D.=10-24 mm were used for fabrication of spouted and fluidized bed reactors. Gaseous products of hydrocarbon decomposition passed through a ceramic filter (for the separation of airborne carbon particles and aerosols) and were directed to a flow meter and GC.

Analysis

The analysis of the products of hydrocarbon decomposition was performed gas chromatographically: SRI-8610A (a thermal conductivity detector, Ar carrier gas, a silica gel column, temperature programming from 25 to 180^{o}C), and Varian-3400, flame ionization detector, He-carrier gas, stationary phase-Hysep D_B. Polynuclear aromatic byproducts were analyzed spectrophotometrically (Shimadzu UV-2401PC). Characterization of carbon products was conducted at Universal Oil Products using SEM, XRD and XPS methods.

Results and Discussion

Decomposition of Hydrocarbons over Carbon Catalysts

This year we continued screening carbon materials of different origin and structure (e.g., activated carbons, carbon blacks, graphites, nanostructured carbons and others) for catalytic activity toward methane decomposition reaction (see Table 1). Testing of all the carbon samples was conducted in the identical experimental conditions (temperature 850^{o}C, methane flow rate 5.0±0.2 ml/min and the amount of carbon sample 0.03±0.001g). This corresponds to a residence time of approximately 1 s in the carbon sample bed. No methane decomposition products other than hydrogen and carbon and very small amounts of C_2 hydrocarbons ($\Sigma C_2 < 0.1$ v.%) were detected in the effluent gas during the experiments. The amount of carbon produced corresponded to the volume of hydrogen within the experimental margin of error (5%). In this paper, all references to the catalytic activity of carbon samples relate to the methane decomposition rate per unit of carbon weight (in mmole/min-g). The control experiments using an inert contact (silica gel with surface area of 600 m^2/g) demonstrated that no appreciable thermal decomposition of methane occurred at these conditions.

Activated carbons (AC) demonstrated the highest initial activity among all of the carbon samples tested. A high initial decomposition rate was followed by a rapid drop in catalytic activity, and, finally, by a quasi-steady reaction rate (in most cases over period of 1-1.5 hours). It is noteworthy that the kinetic curves of methane decomposition over AC samples are quite close to each other despite of the differences in their origin, surface area and method of activation. The initial methane decomposition rates for all the AC samples tested were in the range of 1.63-2.04 mmole/min-g (for the comparison, their surface areas were in much wider range of 650-3370 m^2/g). Experimental data showed no apparent correlation between surface area and the catalytic activity of ACs. Likewise, the origin and method of AC activation had no significant effect on AC catalytic activity in methane decomposition reaction. The initial hydrogen concentration in the effluent gas of AC-catalyzed reaction was in the range of 40-46 v.%. It should be noted, however, that at relatively high residence times (e.g. 10 s in the carbon bed) AC catalysts produced H_2/CH_4 mixtures with the initial hydrogen concentrations reaching up to 90 v.%, which

is an indication of fairly high catalytic activity (comparable with that of Ni- and Fe-based catalysts measured at the identical conditions). The initial rate of methane decomposition over amorphous carbons, e.g. carbon blacks (CB) and acetylene black (AB), was somewhat lower than that of AC samples. CB-catalyzed methane decomposition quickly reached a quasi-steady state rate (over 10-20 min) and remained practically stable for several hours, followed by the gradual decline in the reaction rate. There is a linear dependence between surface area of amorphous carbons (CB and AB) and their relative catalytic activity toward methane decomposition (Figure 3). It is noteworthy that CB and AB were manufactured by different processes (partial oxidation and decomposition, respectively) and from different feedstocks (residual aromatic hydrocarbons and acetylene, respectively).

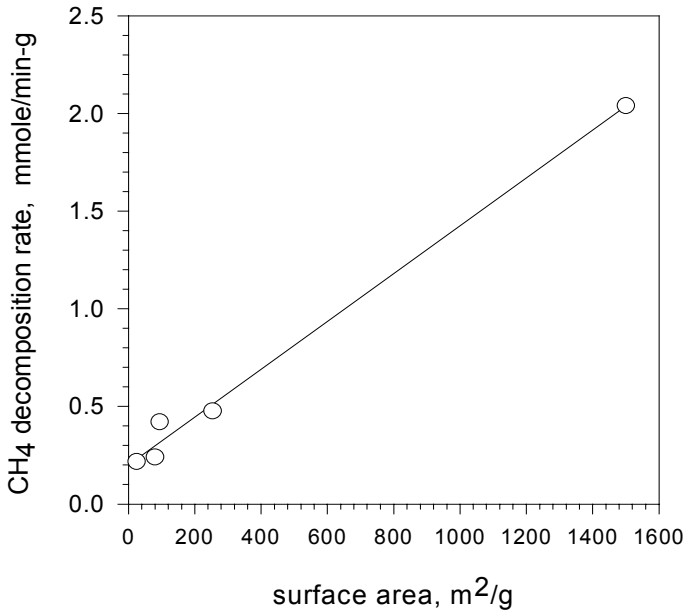

Figure 3. Effect of Surface Area on Methane Decomposition Rate

The above experimental results can be explained as follows. The total rate of the methane decomposition reaction is the sum of the rates of carbon nuclei formation and carbon crystallites growth. The rate of carbon nuclei formation is proportional to the substrate surface area: carbons with high surface area (e.g. ACs and some CBs) tend to have high initial catalytic activity. It was determined that the activation energy of the carbon nuclei formation during methane thermal decomposition (316.8 kJ/mole) is much higher than the activation energy of the carbon crystallites growth (227.1 kJ/mole) (Tesner 1987). Thus, in general, the rate of carbon crystallites growth tends to be higher than the rate of carbon nuclei generation. Rapid deactivation of AC catalysts can be explained by blocking of AC pores by growing carbon crystallites that hinder the internal diffusion of methane molecules. The pore diffusion-controlled reaction could also be responsible for the insensitivity of methane decomposition rate to the origin and surface area of ACs. In contrast, most of the CB surface is relatively easily

accessible to methane molecules during decomposition reaction. CBs differ in particle size, average aggregate mass, morphology, etc. (e.g. the oil furnace process produces CBs with particle diameters in the range of 10-250 nm, and surface area of 25-1500 m^2/g). CBs with high external surface area (e.g. CB BP-2000) result in relatively high steady-state methane decomposition rates. The process could go on for several hours until most of the surface is covered by carbon crystallites produced from methane. It was estimated that it would take almost three hours to cover the surface of CB (BP-2000) with carbon species produced from methane (which is in acceptable agreement with the experiment). After 3-4 hours we observed gradual decrease in methane decomposition rate, due to rapid carbon crystallite growth and reduction in the catalytic surface. Sharp drop in activity of glassy carbon can be explained by the relatively large (comparing to CB) size of particles (3-12 micron), and the lack of open porosity.

In the case of carbon samples with low surface area (graphites, diamond powder, some CBs), the rates of carbon nuclei formation and crystallite growth are likely to become comparable. Low initial methane decomposition rate over natural graphite surface is due to high activation energy of nuclei formation over this material. The increase in hydrogen production rate after the short induction period can be explained by the gradual increase in the surface concentration of catalytically active carbon species produced from methane. It is noteworthy that after 30 minutes the methane decomposition rates over glassy carbon, graphites and synthetic diamond become fairly close. Most likely, from this moment on, the methane decomposition rate is controlled by the catalytic activity of carbon crystallites produced from methane.

Thermocatalytic decomposition of propane over CB catalyst at relatively low residence times (<1s) resulted in pyrolysis gas with relatively high concentrations of ethylene. This can be explained by the thermodynamically favorable reaction (ΔH^o= 81.3 kJ/mol) of the thermal cracking of propane into methane and ethylene. For example, at 800^{o}C and a residence time of approximately 1 s, propane pyrolysis over carbon black CB2000 catalyst resulted in the production of a gaseous mixture with the following composition (vol.%): 52.1%H_2, 38.2%CH_4, 8.5%C_2H_4 and 1.2%C_2H_6. We also conducted a series of experiments on catalytic pyrolysis of a wide range of liquid hydrocarbons (hexane, octane, gasoline and diesel fuel) using different carbon-based catalysts. The quasi steady-state production of the pyrolysis products was achieved over periods of 10-20 min. During gasoline pyrolysis, the gas production yield reached 700 mL per mL of gasoline with an average steady-state hydrogen concentration of approximately 50 v.%.

X-ray diffraction (XRD) studies of the original carbon catalysts and carbon samples produced during propane and methane decomposition were conducted. Carbon black (BP-2000) and activated carbon with the surface area of 1500 m^2/g were used. It was found that the original sample of CB catalyst had one- or, possibly, some two-dimensional ordering, whereas, sample produced from hydrocarbon decomposition had graphite-like ordering in the “columnar” or stacking (003) direction (Figure 4).

The d-spacing (lattice spacing) or spacing between plates is practically uniform, so that the (003) columnar reflection is clearly present. Thus, carbon produced during propane pyrolysis clearly has a typical graphite a-b-c-a type stacking of the carbon ring plates. The actual d-spacing (d =3.4948 Å) of this (003) peak is somewhat larger than that of the standard graphite structure (d =

3.3480 Å), which indicates that the plates are slightly further apart in the columnar stacking direction.

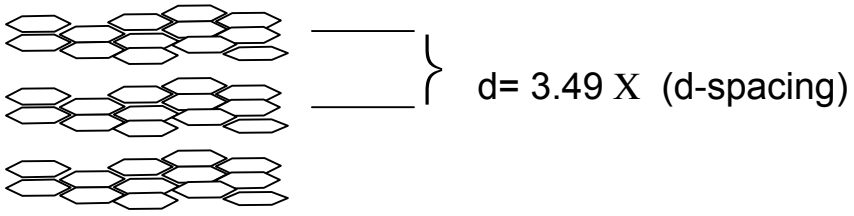

Figure 4. Graphical Representation of Carbon Ring Plates Stacking

Catalyst Stability and Process Sustainability

The development of carbon catalysts featuring long-term stability is one of the major aspects of this work. The experimental results indicated that catalyst deactivation during methane decomposition is common for all types of carbon-based catalysts (although CB is deactivated much slower than AC). It was determined that three chief factors contribute to carbon catalyst deactivation:

1) blocking of catalytically active sites by carbon deposits,
2) surface deposition of catalytically inactive carbon particulates, and
3) reduction in catalytic surface area

Our approach to solving the catalyst deactivation problem is based on an in-situ generation of carbon species catalytically active in the methane decomposition reaction. It is known that the catalytic activity of carbons in methane decomposition is determined by the size of the carbon crystallite and its structure (Tesner 1987). Potentially, the size of carbon crystallites can be affected by the reaction temperature and the presence of other hydrocarbons. The size of the carbon crystallite produced during thermal decomposition of methane is an inverse function of the reaction temperature: the higher the temperature, the smaller the carbon crystallite (Tesner 1987). Figure 5 depicts the correlation between the size of carbon crystallite produced by methane decomposition and the reaction temperature. It is clear that an increase in temperature from 800 to 1100^{o}C would result in only a three-fold reduction in carbon crystallite size. Thus, improvement in catalytic activity of carbon particles via temperature-induced reduction of their crystallite size would require significant increase in methane decomposition temperature (several hundred degrees), which may not be desirable.

We explored the accelerating effect of certain hydrocarbons on the methane decomposition rate as the means of improving long-term stability of carbon catalysts and the sustainability of the process as a whole. It was found that the improvement in the process sustainability can be achieved via in-situ generation of catalytically active carbon particles produced by co-decomposition of hydrocarbons other than methane. We determined the relative catalytic activity of carbons produced by decomposition of hydrocarbons of different classes, e.g. alkanes, unsaturated and aromatic hydrocarbons. Particularly, it was found that carbon produced by

decomposition of unsaturated and aromatic hydrocarbons is catalytically more active than one produced from methane, or other alkanes. Figure 6 demonstrates the accelerating effect of ethylene on the methane decomposition rate.

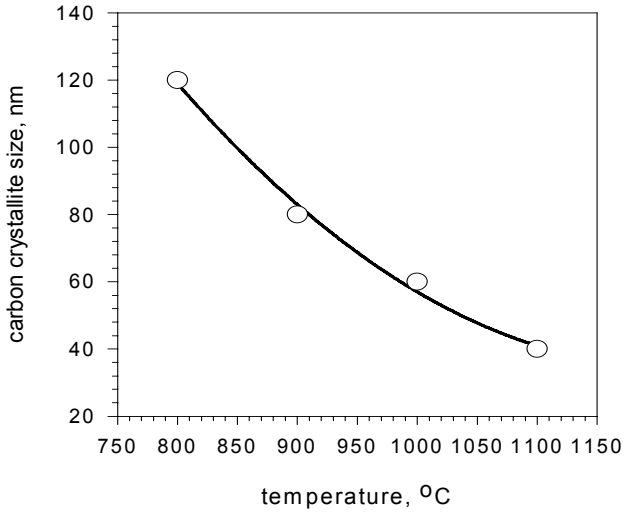

Figure 5. Carbon Crystallite Size as a Function of Temperature

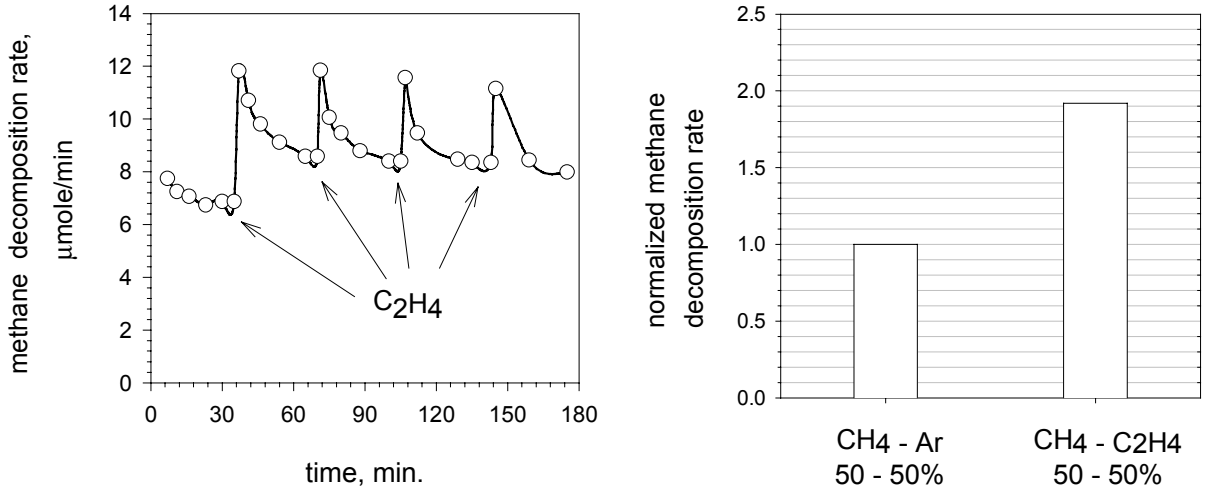

Figure 6. Effect of Ethylene on Methane Decomposition Rate at 850°C

The experiment started with thermal decomposition (850°C) of methane over the surface of activated alumina until quasi steady-state was established (approx. 0.5 h). A pulse of ethylene was introduced into the reactor, followed by rapid purging of the reactor with an inert gas (to remove products of ethylene decomposition), and the introduction of methane into the reactor. We observed a sharp increase (spike) in methane decomposition rate during the first seconds

after methane introduction, followed by its gradual decline to a steady-state level. This procedure was repeated several times, and every time we observed a surge in methane decomposition rate after ethylene pulse (see Figure 6, left). Thus, this experiment proved that carbon produced from ethylene is catalytically more active in methane decomposition than one produced from methane. The accelerating effect of ethylene on the methane decomposition reaction was also demonstrated in a continuous flow experiment using binary CH_4-C_2H_4 (50-50 v.%) mixtures. Particularly, we observed that the rate of methane decomposition over the surface of silica gel at 850^{o}C almost doubles in the presence of ethylene (Figure 6, right). Thus, decomposition of a hydrocarbon with low activation energy (ethylene) induces the decomposition of hydrocarbon with high activation energy (methane).

A similar, even more pronounced effect, was observed when benzene pulses were introduced into the reactor where methane decomposition took place (see Figure 7, left). It was found that the yield of hydrogen produced by the decomposition of methane in a binary mixture with benzene vapor (5 v.%) at 850^{o}C increased almost 8 fold compared to pure methane (after adjusting for the amount of hydrogen produced by benzene) (Figure 7, right).

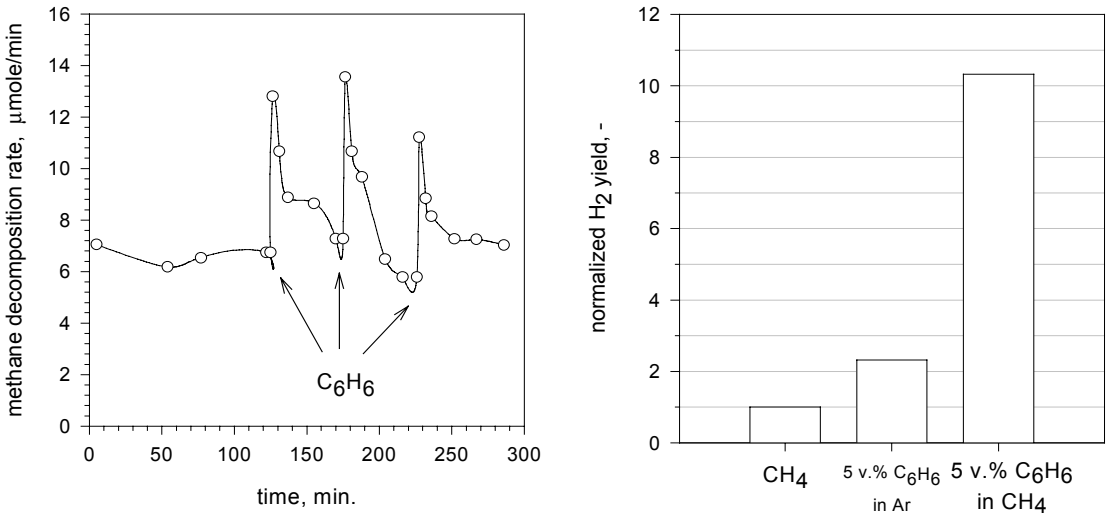

Figure 7. Effect of Benzene Vapors on Methane Decomposition at 850^{o}C

Figure 8 summarizes the relative activity of carbons produced by decomposition of different hydrocarbons in the methane decomposition reaction (normalized against catalytic activity of carbon produced from methane). It was concluded that among all the hydrocarbons tested, carbon produced from aromatics (benzene and naphthalene) exhibited the highest catalytic activity toward methane decomposition.

The relative activity of carbons produced from methane, ethylene and benzene is a linear function of carbon crystallite size in semi-log coordinates (Figure 9).

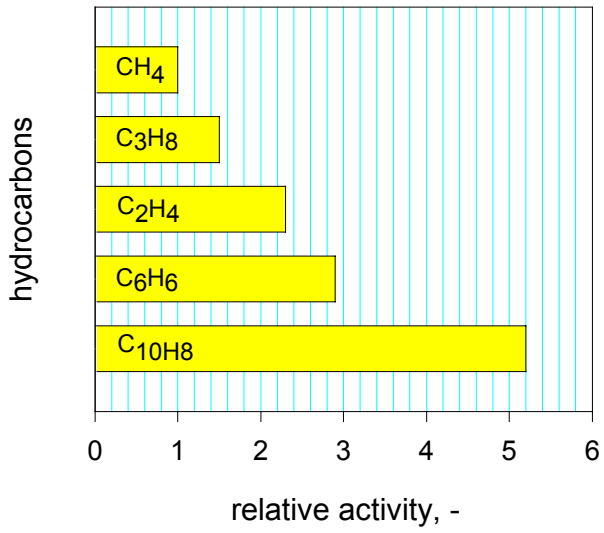

Figure 8. Relative Activity of Carbons Produced from Different Hydrocarbons in Methane Decomposition Reaction at 850°C

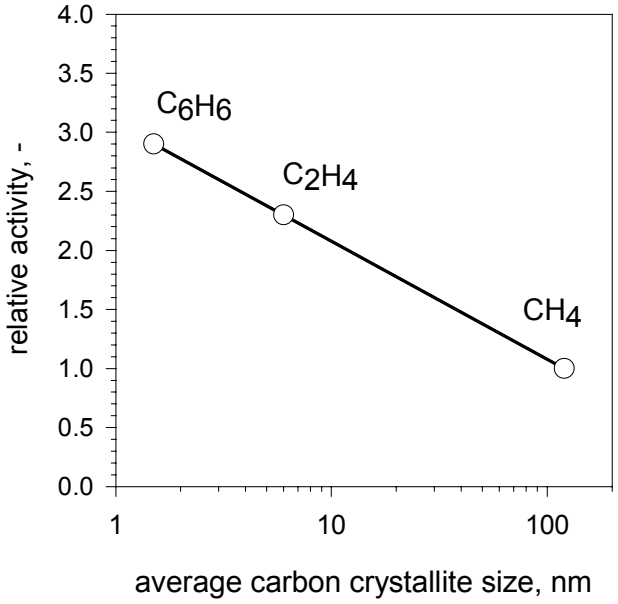

Figure 9. Relative Activity of Carbons Produced from Methane, Ethylene and Benzene as a Function of Carbon Crystallite Size

These data have important implications on improvement of the process sustainability of the hydrocarbon decomposition process. At relatively high space velocities, noticeable amounts of ethylene and aromatics are present in the gases of propane and methane-propane pyrolysis. Thus, recycling pyrolysis gas (with olefins and aromatics) back to the reactor after separation of hydrogen could significantly improve the long-term stability of carbon catalyst and the process sustainability.

Catalytic Reactors for Decomposition of Hydrocarbons

The selection of a catalytic reactor suitable for the efficient decomposition of methane (or other hydrocarbons) with continuous withdrawal of the product carbon from the reactor is another important aspect of the process development. During Phase I work, we looked upon several types of reactors potentially suitable for the production of hydrogen and continuous withdrawal of carbon, such as a tubular, a fluid wall, and a free-volume reactor. Unfortunately, these reactors featured very high temperatures (in excess of 1000°C) and low methane conversions. Fixed (or packed) bed catalytic reactors were used in our studies to rapidly screen the catalytic activity of carbon samples. However, continuous adding to or withdrawal of carbon from a fixed bed reactor could present a daunting technical problem. This year we continued studies on the development (or selection) of reactors suitable for the production of hydrogen-rich gas with simultaneous withdrawal of carbon from the reactor at moderate temperatures (< 900°C). The reactors under consideration were spouted and fluidized bed catalytic reactors. We fabricated micro-reactors of each type and tested them for the simultaneous production of hydrogen and carbon using methane and propane as feedstocks.

Spouted bed reactor

In a spouted bed reactor (SPR) hydrocarbon feedstock enters from the small nozzle at the base of the catalytic bed at high velocity, creating a central dilute phase core (Figure 10). The carbon particulates rise inside the core forming a fountain. Hydrocarbon flows mainly inside the core, although some percentage of the flow might be distributed to the peripheral annular region (annulus). We fabricated a small-size SBR and tested it for methane decomposition in the presence of carbon black (BP-2000) in temperature ranges of 800-1000°C.

Before the actual methane decomposition experiments we ran "cold" experiments to visually determine the optimum gas velocity for carbon particles spouting. It was found that an adequate spouting of carbon black particles by the stream of methane could be achieved at the superficial gas velocity of 2 cm/s and a bed depth to a reactor diameter ratio of 5-6. At higher values of superficial gas velocities and depth-to-diameter ratios, we observed a non-homogeneous fluidization of carbon particles. Applying the above conditions to the methane decomposition experiments (at 900°C) we observed fairly poor conversion of methane (7%). This could be attributed to very short contact time between carbon particles and hydrocarbon within the spouting region. The contact time in the spout was estimated by calculating mean spout diameter according to the following equation (Mathur 1974):

$$D_s = \frac{0.118 G^{0.48} D_c^{0.68}}{\rho_b^{0.41}}$$

where: D_s is the spout diameter (cm), G is the methane mass flow rate per unit of reactor cross section (g/sec-cm^2), D_c is the reactor diameter (cm), and ρ_b is the carbon bulk density (g/cm^3).

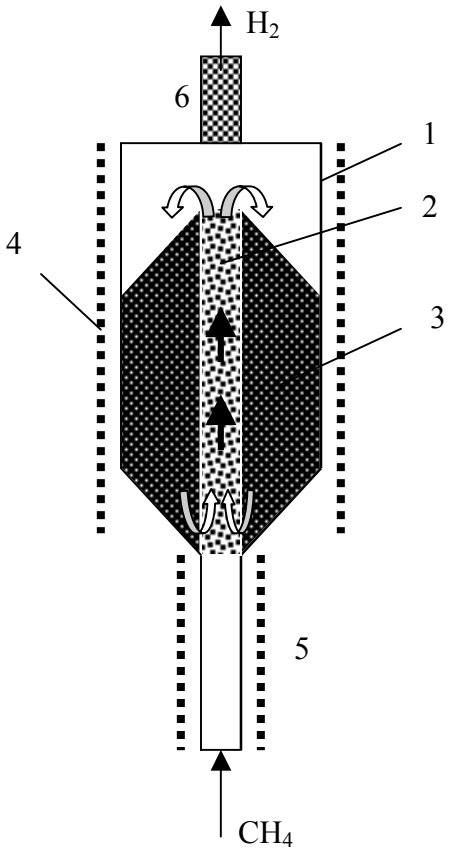

Figure 10. Spouted Bed Reactor

1- external wall of the reactor
2- spouting zone
3- catalyst
4- electric heater
5- pre-heater
6- filter

The calculation yielded a residence time of approximately 0.1 s within the spouting region. Although intense turbulence makes for high coefficients of heat and mass transfer, the effect would be minimal due to the very small residence time in the reaction zone (which would be very difficult to control). Thus, very short contact times intrinsic in the operation of SBRs could result in relatively low methane conversion rates. It should be noted that due to inequality of contact times in the spout and annulus of the SBR, the extent of the reaction taking place in these regions would also be unequal, which might present a problem with modeling the reactor.

Another potential problem is associated with the size of carbon particles. According to (Mathur 1974), the minimum particle diameter for which spouting appears to be practical is about 1 mm, which by far exceeds the expected range of carbon particle sizes in our process (estimated at 10-100 microns). These considerations weigh heavily against the use of SBR for NG decomposition in a large scale units.

Fluidized Bed Reactor

Fluidized bed reactors (FBR) have been widely used in the chemical, metallurgical and petroleum industries. A fluidized bed system does provide constant flow of solids through the reaction zone, which makes it particularly suitable for the continuous addition and withdrawal of carbon particles from the reactor (similar to fluid catalytic cracking process). In an FBR, the bed of fine carbon particles behaves like a well-mixed body of liquid giving rise to high particle-to-gas heat and mass transfer rates. During fluidization, carbon particles are allowed to spend a certain time in the reaction zone, which could be easily controlled by adjusting the ratio between the feed rate and the weight of the bed. The bed could also buffer any instabilities that arise during continuous operation.

A schematic diagram of FBR used in our experiments is shown in Figure 11. Preheated to 400^{o}C a stream of methane (or propane, or methane-propane mixture) entered the FBR from the bottom, and contacted with the fluidized bed of carbon particles (carbon black BP-2000) at 800-950^{o}C in the reaction zone, where pyrolysis of hydrocarbons occurred.

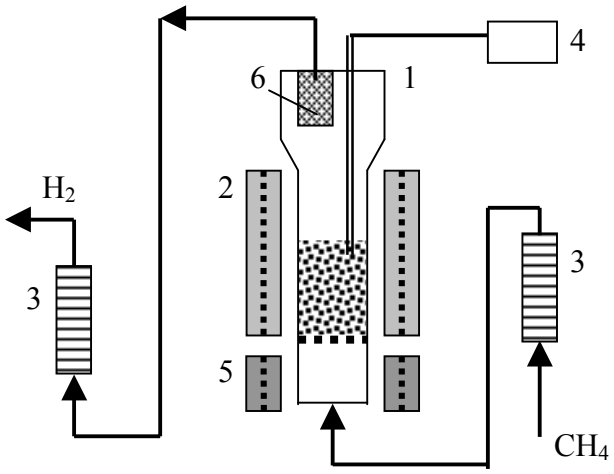

Figure 11. Fluidized Bed Reactor

1- fluidized bed reactor
2- electric heater
3- flow meter
4- temperature controller
5- pre-heater
6- filter

The minimum methane flow rate necessary for fluidization of carbon particles was found from the following equation (Othmer 1956):

$$G = \frac{0.005 d_p{}^2 \varepsilon^3 (\rho_p - \rho_f) \rho_f g}{\psi^2 (1-\varepsilon) \mu}$$

where: G is the mass flow rate necessary to initiate fluidization, d_p is the diameter of the particle (cm), ε is the fraction voids, ρ_p is the density of particle (g/cm^3), ρ_f is the density of methane (g/cm^3), g is the acceleration gravity (cm/s^2), ψ is the shape factor, μ is the viscosity (g/cm.s)

The flow of hydrogen-containing gas exited from the top of the reactor through a ceramic filter and was directed to a gas chromatograph.

Figures 12 depicts the kinetic curves of decomposition of methane, propane and their mixtures (3:1 by volume) over CB catalyst at 850 and 950^{o}C. Propane was almost quantitatively converted into hydrogen-rich gas, whereas, methane decomposition yields were somewhat lower. The propane pyrolysis gas was rich in ethylene and other heavier hydrocarbons. Thus, the experimental results indicated that a gas with the hydrogen concentration in the range of 40-50 v.% could be produced from methane and methane-propane mixtures in a quasi steady-state regime using fluidized bed of BP-2000 particles.

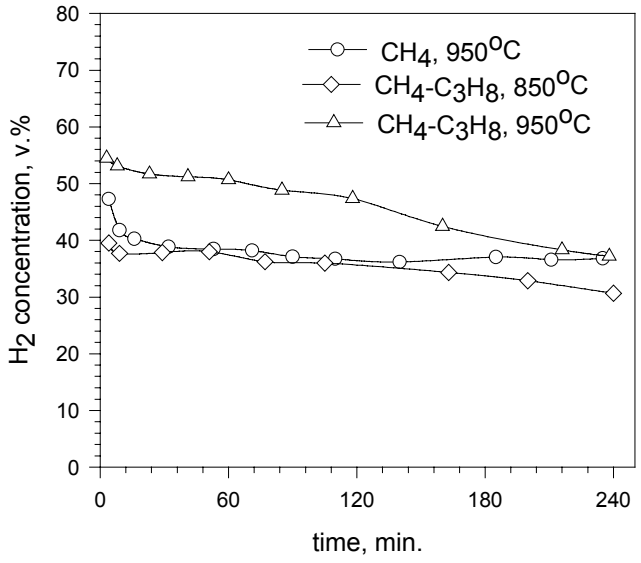

Figure 12. Methane and propane decomposition over CB (BP2000) using fluidized bed reactor

It can be seen from the Figure 12 that after 1.5-2 hours, hydrocarbon decomposition rates started to drop, which could be explained by the decrease in the catalytic surface area. Indeed, at the end of experiment we observed the accumulation of coarse (0.1-1 mm in diameter) carbon particles in the bottom section of the reaction zone.

Technological Scheme of Thermocatalytic Process

Based on the above experimental data, we proposed the following technological scheme for the thermocatalytic decomposition (TCD) process. Figure 13 shows the simplified schematic diagram of the TCD process. A fluidized bed catalytic reactor (1) and a fluidized bed heater (2) are the two main pieces of equipment in the process. For the sake of simplicity, auxiliary equipment such as compressors, cyclones, and others are not shown in the figure. A preheated stream of a hydrocarbon feedstock enters the reactor (1) where it is decomposed (pyrolyzed) at temperatures of 850-900^{o}C, and pressure of 100-500 kPa over the fluidized bed of catalytically active carbon particulates. The resulting hydrogen-containing gas is directed to a cyclone, a heat exchanger (3), and, finally, to a gas separation unit (4), where a stream of hydrogen with the purity of >99.0 v.% is separated from the gaseous stream. The gas separation unit could be a membrane or pressure-swing adsorption (PSA) unit. The concentration of hydrogen in the effluent gas after the reactor (1) depends on the hydrocarbon feedstock, the temperature and the residence time in the reactor and varies in the range of 40-60 v.%, with the balance being methane and higher hydrocarbons (C_2+, including ethylene and other unsaturated and aromatic hydrocarbons). The non-permeate gas (or PSA off-gas), consisting of CH_4 and C_2+ hydrocarbons, is recycled to the catalytic reactor. The concentration of gaseous olefins in the non-permeate gas (or off-gas) depends on the feedstock and could reach up to 20 v.%. As discussed earlier, decomposition of unsaturated and aromatic hydrocarbons produce carbon species catalytically active in the methane decomposition reaction. Thus, recycling the non-permeate gas (or PSA off-gas) containing olefins and aromatic hydrocarbons back to the reactor allows one to sustain the thermocatalytic process via in-situ generation of catalytically active carbon species.

Product carbon (coke) is withdrawn from the bottom of the fluidized bed reactor in the form of carbon particulates with the size of >100 microns. Approximately half of carbon is ground into fine (<100 microns) powder in a grinder (5), and directed to a heater (2) where it is heated to 900-1000^{o}C. The hot carbon particles from the heater flow down to the top of the reactor bed. A jet attrition system in the reactor provides additional seed carbon particles to maintain a constant particle size within the system (approximately 100 micron). The heat input necessary to drive the endothermic process could be provided by burning a portion of carbon with air in a heater. Alternatively, heat could be provided by combusting either a part of the hydrocarbon feedstock, or a portion of the recycle. Ash-, sulfur- and metal-free carbon is a valuable byproduct of the process that could significantly reduce the cost of hydrogen production by TCD process. Thus, in general, the technological chain of the process is similar to that of the fluid coking process, which has been successfully operated since 1950's.

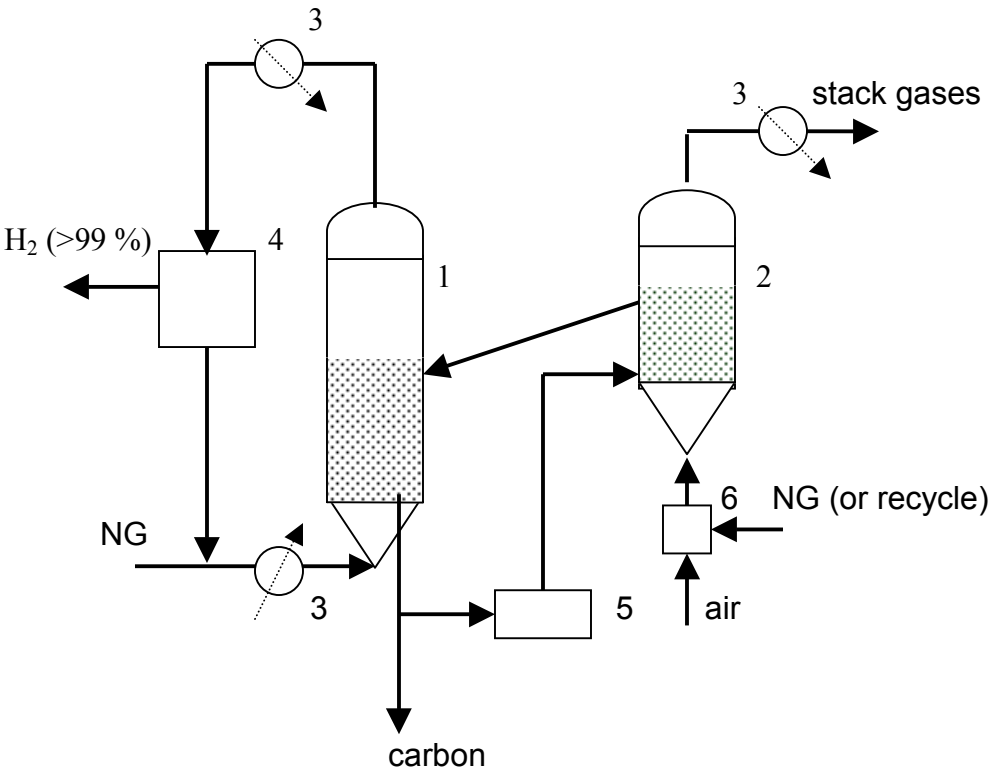

Figure 13. Simplified Schematic Diagram of Thermocatalytic Process 1- reactor, 2- heater, 3- heat exchanger, 4- gas separation unit, 5- grinder, 6- combustor

Reactors for Small Scale Hydrogen Production

Miniature (10 W) Hydrogen Generator

We have been working on the development of the reactors for small-scale hydrogen production. The concept is based on the catalytic decomposition of liquefied or liquid hydrocarbon fuels that act as irreversible chemical "hydrides." For example, gravimetric densities of hydrogen in propane and gasoline are equal to 18.2 and 13.4 w.%, respectively, which by far exceed that of all known metal hydrides and nano-carbon systems. Furthermore, the reactor does not produce CO, which obviates the need for WGS and other gas conditioning stages. This may potentially result in a compact hydrogen generator operating on a wide range of hydrocarbon fuels, e.g. LPG, gasoline, kerosene and diesel fuel. To demonstrate the technical feasibility of this concept we designed and fabricated a 10 W_{th} hydrogen generator (Figure 14).

Figure 14. A 10 W Hydrogen Generator

The hydrogen generator has a tubular design (OD=2.5 cm and length of 15 cm) (the design of the generator is proprietary; a patent application has been filed with U.S. PTO). It has been tested using commercial gasoline and diesel fuel as feedstocks (the fuels were pre-dried before the experiments). The hydrogen generator produced a gaseous stream consisting of hydrogen and methane as a major and a minor component, respectively. No CO or CO_2 were detected in the gas produced by the hydrogen generator. In the case of gasoline, the hydrogen-rich gas was produced at the average production rate of 10 ml/min and the following composition (v.%): 76.3% H_2, 23.7% CH_4, with trace amounts of C_2^+ hydrocarbons. Based on the hydrogen yield, the specific energy (SE) achieved in this system was estimated at 2.3 $kW_{th}h$ per kg of fuel (the external source of energy for the heating is not included). Coupling of this reactor with a PEM FC (at PEM efficiency of 50%) would result in SE of the entire power system close to 1 $kW_{el}h$ per kg of fuel. This value of SE is three times higher than that of the advanced methanol/water reformer (300 Wh per kg of fuel) reported in the literature (Fuel Cell Industry Report 2000). The portable power systems (10-50 W range) based on the combination of a compact hydrogen generator with a fuel cell can find important applications in many areas, particularly in "soldier power" systems, as it lacks acoustic and chemical "signatures."

1 kW Hydrogen Generator

We have designed and fabricated a 1 kW_{th} hydrogen generator. Similar to the 10 W hydrogen generator, its operation is based on thermocatalytic pyrolysis of hydrocarbon fuels over carbon-based catalysts. Since no carbon oxides are produced during catalytic decomposition of hydrocarbon fuels, the hydrogen gas can be directly fed into a polymer electrolyte membrane (PEM) fuel cell without need for water-gas shift, preferential oxidation and CO_2 separation stages. Figure 15 demonstrates the experimental set-up consisting of 1 kW hydrogen generator, a propane tank, a PEM fuel cell and testing equipment.

A PEM fuel cell has been provided by the Energy Partners, and the fuel cell testing equipment was purchased from Scribner Assoc. The results of the hydrogen generator testing (without connecting it to a fuel cell) are presented in Figure 16. In the first series of experiments, propane was introduced into the hydrogen generator at different flow rates. Figure 16 (left) demonstrates the distribution of propane pyrolysis products as a function of the effluent gas flow rate. Hydrogen concentration in the pyrolysis gas reached almost 80 v.% at lower flow rates, and it dropped to approximately 70 v.% as the effluent gas flow rate increased from 1.2 to 5.1 L/min. The balance was methane with the traces of ethane. No appreciable amounts of carbon oxides or other reactive gases were detected in the pyrolysis gas.

Figure 15. Hydrogen Generator Connected to Propane Tank, PEM Fuel Cell and Testing Equipment

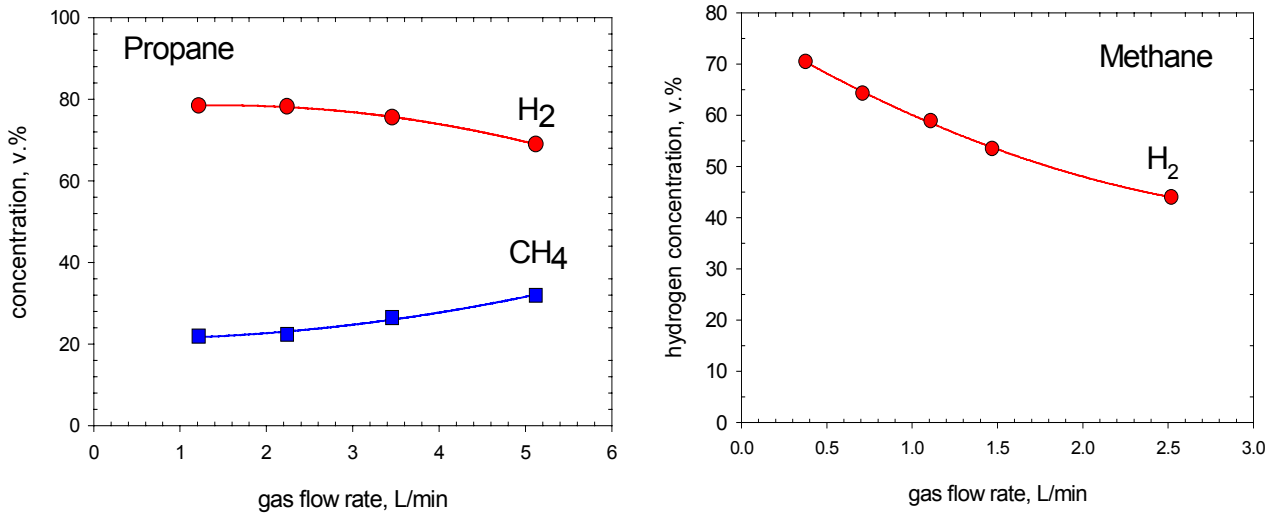

Figure 16. Production of Hydrogen-rich Gas from Propane (left) and Methane (right) Using 1 kW Hydrogen Generator

As expected, methane produced a gas with somewhat lower concentrations of hydrogen (Figure 16, right.) At low flow rates, the concentration of hydrogen in methane decomposition gas was 70 v.%; however, it dropped to 45 v.% at high flow rates (2.5 L/min) of the effluent gas. Again, no carbon oxides were detected in the gaseous stream exiting the hydrogen generator.

Status of Economics

Technoeconomic analysis of thermocatalytic decomposition of natural gas was conducted by NREL, based on the experimental data input provided by FSEC. The details of the analysis will be published in NREL's report (Lane and Spath 2001). Courtesy of NREL, we present selected results of the analysis related to one particular process design that included a fluidized bed catalytic reactor and a fluidized bed heater with carbon particles circulating between these two apparatuses (similar to the schematic presented in Figure 13). Process heat is provided by combusting part of the NG and carbon. A PSA unit was assumed for the production of high purity hydrogen (>99 v.%). Three plant sizes were analyzed (in MMscfd): small- 6, medium- 20 and large- 60. The analysis assumed the internal rate of return of 15%. Figure 17 demonstrates hydrogen selling price as a function of natural gas selling price for three hydrogen plants (assuming a carbon selling price of $300/t).

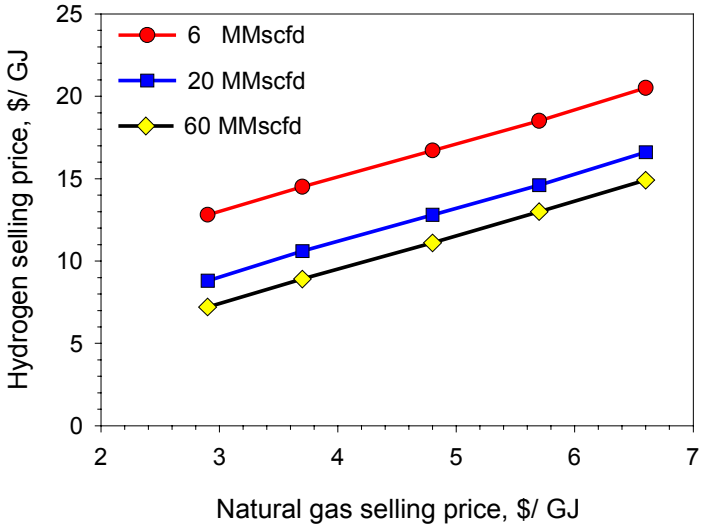

Figure 17. Hydrogen Selling Price vs Natural Gas Selling Price

At natural gas prices ranging from $2.9 to 6.6 per GJ, the hydrogen selling price varied in the range of $7.2-14.9 /GJ for a large plant, and $12.8–20.5/ GJ for a small plant. It should be noted that hydrogen selling prices would be further reduced if a carbon credit for avoided CO_2 emissions were applied.

The sensitivity analysis on the effect of the carbon selling price on the hydrogen selling price was also conducted. Figure 18 shows the plots: hydrogen selling price vs carbon selling price for the small, medium and large hydrogen plants at a NG price of $3.72 per GJ. It is evident that carbon credit significantly reduces the cost of hydrogen production. Particularly, at carbon selling prices ranging from $0 to 500 per metric ton, the plant gate hydrogen selling price varies from $13.8 to 5.7/GJ, for the large plant, and from $19.4 to 11.2/GJ, for the small plant.

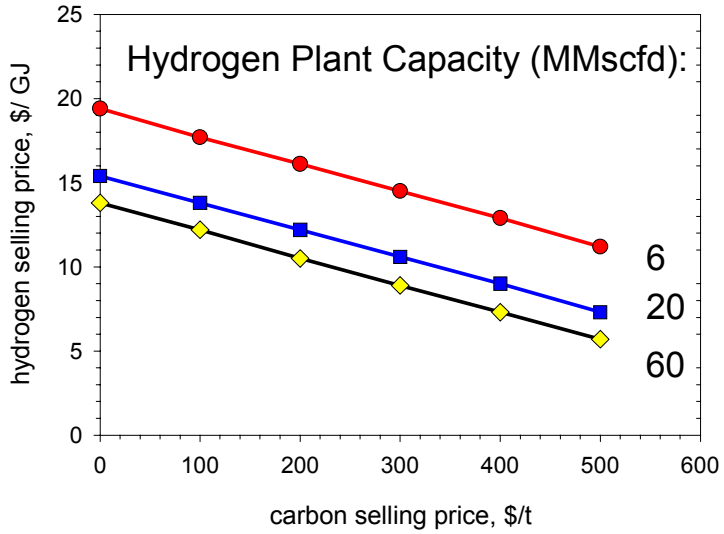

Figure 18. Hydrogen Selling Price vs Carbon Selling Price

Since carbon credit markedly affects the economics of the TCD process, a great deal of consideration was given to the characterization of the carbon product and estimation of its market value. This work was conducted in cooperation with the Universal Oil Products (UOP) (Des Plaines, IL). UOP has conducted SEM, XRD and XPS analysis of carbon produced by catalytic pyrolysis of propane and methane over carbon black catalyst. In general, the results of XRD analysis conducted by UOP were in an agreement with the results of the prior analysis of carbon samples, conducted by AMIA Laboratories (Rigaku) (see Phase I Report). It was inferred that the carbon produced by TCD process revealed a graphite-like structure. It was also concluded that carbon produced in the process could be suitable for the production of electrodes in the aluminum and ferro-alloy industries. Currently, the aluminum industry produces annually close to 4 mln tons of aluminum, with a carbon (coke) consumption rate of 0.4-0.5 kg of carbon per kg of Al (Kirk-Othmer 1992). Thus, the aluminum industry could be a very important market for sulfur- and metal-free carbon produced in TCD process with the selling prices of $300 per ton and higher.

Comparative Assessment of TCD and SR Processes

We have conducted a comparative economic assessment of TCD (with and without carbon credit) and SR (with and without CO_2 sequestration) processes (Figure 19).

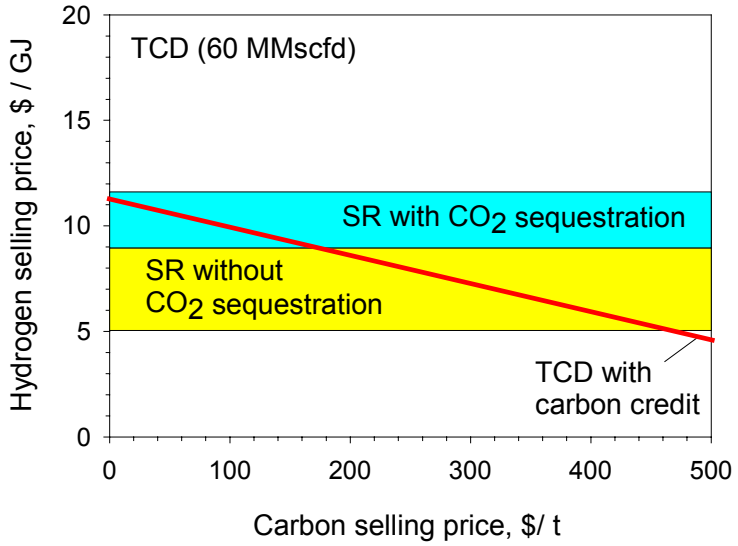

Figure 19. Comparative Economic Assessment of TCD and SR

The comparison is based on a large capacity hydrogen plant and a NG price of about $3/GJ. The cost of hydrogen production by a large SR plant was estimated at $5-9/GJ (Ogden et al. 1997). It was assumed that the total cost of hydrogen production by SR plant coupled with CO_2 sequestration would increase by 25-30% (Audus et al. 1996). For the purpose of this comparative assessment, sequestration of CO_2 from TCD process is not considered (it was assumed that upon the optimization of TCD process, CO_2 emissions from it would be minimal compared to those from SR). It is evident from the Figure 19 that the cost of hydrogen production by TCD process becomes comparable with that of SR process (without CO_2 sequestration) if carbon is sold at the price range of approximately $160-460 per ton. However, if strict environmental restrictions on CO_2 emissions are imposed in future, and CO_2 sequestration from SR process becomes mandatory, hydrogen selling prices for SR and TCD will be comparable, even without carbon credit.

Conclusion

Thermocatalytic decomposition of NG (or other hydrocarbon fuels) as a viable technological approach to the production of hydrogen and solid carbon is discussed in this paper. Decomposition (or pyrolysis) of hydrocarbons occurs in the presence of catalytically active carbon particles at moderate temperatures (<900^{o}C) in an air/water-free environment, which

eliminates the concurrent production of carbon oxides. The advantages of TCD process can be summarized as follows: (i) it is technologically simple (only one chemical stage); (ii) clean carbon is produced as a valuable byproduct; and (iii) CO_2 emissions from the process are significantly reduced. Phase II work focuses on the long-term catalyst stability and process sustainability, and other technological aspects of the TCD process development. Factors affecting carbon catalyst activity and stability were investigated. It was determined that the catalyst stability and process sustainability can be improved via in-situ generation of catalytically active carbon species. Several types of reactors, including spouted and fluidized bed reactors were evaluated for hydrocarbon decomposition process. A fluidized bed reactor was selected as the most suitable for the efficient decomposition of methane and propane with the production of hydrogen-rich gas and simultaneous withdrawal of carbon from the reactor. Reactors for small-scale production of hydrogen (at 10 W and 1 kW range) have been designed, fabricated and tested. It was found that a wide range of hydrocarbon fuels, including methane, propane, gasoline and diesel fuel could be efficiently converted into a gas with hydrogen concentration up to 80 v.%, with the balance being methane. Since this gas does not contain carbon oxides or other reactive impurities, it could be directly fed to any type of fuel cell, including CO-sensitive PEM fuel cells. The technoeconomic analysis conducted by NREL demonstrated that the TCD process could be economically advantageous if credits for the product carbon and avoided CO_2 emissions were applied.

The ecological advantages of TCD over other processes become more appreciable if applied to small-scale hydrogen plants for on-site (or decentralized) production of hydrogen. It was concluded by the authors of recent technical reports that the sequestration of CO_2 produced by decentralized SR hydrogen plants would not be economical, since it would require building of an expensive CO_2 infrastructure (Ogden et al. 1997 and Sokolow, Ed. 1997). This implies that all the CO_2 produced at decentralized SR hydrogen plants will be vented into the atmosphere. In contrast to that, solid carbon produced by TCD process could be easily handled by means of truck shipping to an end-user or to a disposal site without the necessity of building a new infrastructure.

New markets for carbon-based products will most likely be developed in the near future. For example, it is conceivable that carbon-based materials would eventually replace (at least, partially) many major building and construction materials, and, most importantly, cement. This would result in even further reductions in overall CO_2 emissions due to phasing out of cement manufacturing plants, which are major industrial CO_2 producers. Although the market for carbon-based materials is continuously growing, it is possible that not all the carbon produced by TCD process will be absorbed by the traditional and perspective application areas. In this case all the remaining carbon would be sequestered or stored for the future use. Carbon is an inert material under ambient conditions, so it can be conveniently and safely stored for the extended periods of time (in landfills or depleted mines) with minimal ecological uncertainties.

Future Work

- Collaborate with industry to scale up and optimize the process with respect to throughput, hydrogen purity and reduced greenhouse gas emissions

- Design and fabricate a process development unit and evaluate its performance using technical-grade hydrocarbon fuels
- Demonstrate active operation of the thermocatalytic reactor coupled with a PEM fuel cell
- Address safety issues related to operation of the reactor and handling the carbon product
- Demonstrate tolerance to moisture, sulfur and other impurities present in commercial hydrocarbon fuels
- Increase specific energy of the thermocatalytic reactor
- Work with industry to identify the areas of applications for the carbon product; evaluate new markets for carbon

Acknowledgements

This work was supported by the U.S. Department of Energy under the contract No. DE-FC36-99GO10456 and the Florida Solar Energy Center (University of Central Florida). The author also acknowledges the contribution of the Universal Oil Products, National Renewable Energy Laboratory, Energy Partners, Florida Institute of Technology, and AMIA Laboratories (Rigaku).

References

Audus, H., O. Kaarstad, and M. Kowal. 1996. "Decarbonization of Fossil Fuels: Hydrogen as an Energy Carrier". In *Proceedings of 11th World Hydrogen Energy Conference*, 525. Stuttgart, Germany.

Blok, K., R. Williams, R. Katofsky, and C. Hendriks. 1997. "Hydrogen Production from Natural Gas, Sequestration of Recovered CO_2 in Depleted Gas Wells and Enhanced Natural Gas Recovery". *Energy*, 22: 161-168

Calahan, M. 1974. "Catalytic Pyrolysis of Methane and other Hydrocarbons". In *Proceedings of Conference on Power Sources.* 181

Fuel Cell Industry Report. 2000. 1: No.4

Fulcheri, L., and Y. Schwob. 1995. "From Methane to Hydrogen, Carbon Black and Water". *Int. J. Hydrogen Energy,* 20: 197.

Gaudernack, B., and Lynum S. 1996. "Hydrogen from Natural Gas without Release of CO_2 to the Atmosphere". In *Proceedings of 11th World Hydrogen Energy Conference,* 511-523. Stuttgart, Germany.

Kirk-Othmer Encyclopedia of Chemical Technology. 1992. New York, John Wiley & Sons

Lane, J. and P.Spath. 2001. *Technoeconomic Analysis of the Thermocatalytic Decomposition of Natural Gas,* NREL Technical Report. Golden, CO.

Mathur, K. and N. Epstein. 1974. *Spouted Beds*, New York, Academic Press

Muradov, N. 1993. "How to Produce Hydrogen from Fossil Fuels without CO_2 Emission". *Int. J. Hydrogen Energy*, 18: 211

Ogden, J., M. Steinbugler and T. Kreutz. 1997. "Hydrogen as a Fuel for Fuel Cell Vehicles: a Technical and Economic Comparison". In *Proceedings of the 8th Annual U.S. Hydrogen Meeting,* Alexandria, 469. VA

Othmer, D. (Ed.). 1956. *Fluidization.* New York; Reinhold Publ.

Pourier, M. and C. Sapundzhiev. 1997. "Catalytic Decomposition of Natural Gas to Hydrogen for Fuel Cell Applications". *Int. J. Hydrogen Energy*, 22:429

Perkins, S. 2000. *Science News*, 158: 396.

Socolow, R. (Ed.). 1997. "Fuels Decarbonization and Carbon Sequestration". Report of a Workshop. PU/CEES Report No. 302, Princeton University

Steinberg, M. 1999. "Fossil Fuel Decarbonization Technology for Mitigating Global Warming". *Int. J. Hydrogen Energy*, 24: 771

Tesner, P. 1987. *Kinetics of Pyrocarbon Formation*. Moscow; VINITI.